Nuclear Engineering and Technology 49 (2017) 865–872

Contents lists available at ScienceDirect

Nuclear Engineering and Technology

journal homepage: www.elsevier.com/locate/net

Technical Note

High-power fiber laser cutting parameter optimization for nuclear Decommissioning

Ana Beatriz Lopez [a, *], Eurico Assunção [a, b], Luisa Quintino [a, b], Jonathan Blackburn [c], Ali Khan [c]

[a] IDMEC, Instituto Superior Técnico, Universidade de Lisboa, Lisboa, Portugal
[b] European Federation for Welding, Joining and Cutting, Porto Salvo 2740-120, Portugal
[c] TWI Ltd., Granta Park, Cambridge, CB21 6AL, UK

ARTICLE INFO

Article history:
Received 15 July 2016
Received in revised form
31 December 2016
Accepted 2 February 2017
Available online 24 February 2017

Keywords:
Decommissioning
Fiber Laser Cutting
High-power Lasers
Kerf Width Analysis
Nozzle Combinations
Nuclear Facilities

ABSTRACT

For more than 10 years, the laser process has been studied for dismantling work; however, relatively few research works have addressed the effect of high-power fiber laser cutting for thick sections. Since in the nuclear sector, a significant quantity of thick material is required to be cut, this study aims to improve the reliability of laser cutting for such work and indicates guidelines to optimize the cutting procedure, in particular, nozzle combinations (standoff distance and focus position), to minimize waste material. The results obtained show the performance levels that can be reached with 10 kW fiber lasers, using which it is possible to obtain narrower kerfs than those found in published results obtained with other lasers. Nonetheless, fiber lasers appear to show the same effects as those of CO_2 and ND:YAG lasers. Thus, the main factor that affects the kerf width is the focal position, which means that minimum laser spot diameters are advised for smaller kerf widths.

© 2017 Korean Nuclear Society, Published by Elsevier Korea LLC. This is an open access article under the CC BY-NC-ND license (http://creativecommons.org/licenses/by-nc-nd/4.0/).

1. Introduction

The laser process has been studied for dismantling work for more than 10 years. Among the cutting processes available, the one using a multikilowatt laser is the most commonly investigated process. Developments and tests with a pulsed YAG laser and a CO_2 laser, for which the maximum average power output levels were 1.2 kW and 5 kW, respectively, have been performed for the nuclear sector. In addition, Chagnot et al. [1] performed recent studies to assess the performance of high-power (up to 8 kW) Nd:YAG lasers. Other thick cutting developments with high-power lasers not dedicated to the nuclear industry have been addressed [2, 3].

Fiber laser technology has many advantages compared with carbon dioxide laser technology. Specifically, the advent of high-power (4+ kW) lasers has provided a realistic opportunity for the use of lasers in decommissioning applications. The development of such lasers has further enhanced decommissioning capability by providing scalable power in the multikilowatt regime with significantly better beam quality. Furthermore, power can be transmitted via several hundred meters of fiber-optic cable, and hence the laser unit can be located some distance away from the active area of operations. Moreover, low maintenance costs, high efficiency, and small implantation space are advantages of this process [4]. However, the main disadvantages of fiber compared with CO_2 lasers relate to the efficiency when processing thicker materials, typically those with a thickness above 5 mm.

In fact, in the nuclear sector, a significant quantity of thick material needs to be separated effectively. The objective, in such types of work, is to minimize the kerf width in order to achieve minimum material loss and reduce energy requirements [5]. Physical processes involved in laser cutting of thick sections are complex. It is known that laser parameters, in particular laser power, focus settings, cutting speed, and assisting gas and its pressure, influence the physical processes in the cutting section. It was found that the higher the power intensity and the gas pressure, the higher the thermal erosion in the kerf [3] and also the thickness that can be cut.

Furthermore, it is well known that to cut materials of larger thickness, the laser power must increase and the cutting speed must decrease to maximize the heat input [5]. However, recent studies on high-power laser cutting have indicated that different focusing lenses do not affect cutting characteristics [6].

* Corresponding author.
E-mail address: beatriz.mendes.lopez@gmail.com (A.B. Lopez).

http://dx.doi.org/10.1016/j.net.2017.02.004
1738-5733/© 2017 Korean Nuclear Society, Published by Elsevier Korea LLC. This is an open access article under the CC BY-NC-ND license (http://creativecommons.org/licenses/by-nc-nd/4.0/).

Despite the existence of a significant number of publications related to high-power lasers, almost no data are available concerning the capabilities of such lasers for use in decommissioning applications to cut thick sections. Nevertheless, it will be interesting to understand what is already known about minimizing material losses and energy requirements. Therefore, to determine the feasibility of using this technique in the nuclear sector, a review of progress in the area of high-power lasers is presented below. In addition, a brief explanation of the laser interaction parameters, as well as of the concept of management of laser beam energy and kerf width, will be given.

First is the specific point energy concept. Three basic laser interaction parameters have been analyzed in current studies focusing on laser welding [7]: power density, interaction time, and specific point energy (SPE). These parameters allow the welding process to be defined in order to obtain a given depth of penetration and weld width. Moreover, it was found that such parameters are applicable to laser cutting. Although there has been no research addressing the effect of these parameters on thick steel, it may be useful to investigate whether or not the SPE concept fits in this work.

Power density is calculated using the following equation:

$$Power\ Density = \frac{P}{A_{(beam)}} \tag{1}$$

where P is the power and $A_{(beam)}$ is the area of the laser beam.

Interaction time is given by the following equation:

$$t_i = \frac{d_b}{V} \tag{2}$$

where d_b is the beam diameter and V is the cutting speed. The interaction time can be interpreted as the heating time of the process on the centerline of the weld, or, in the case of laser cutting, as the interaction time between the laser and the material [8]. The energy delivered to the material in the interaction time, termed the SPE, can be calculated as follows:

$$S_{PE} = Power\ Density{*}t_i{*}A_{(beam)} \tag{3}$$

This parameter allows a comparison between beams of different diameters [8]. The study of these parameters has showed that, in laser cutting, the depth of penetration is controlled by power density, and the SPE and kerf width are mainly controlled by beam diameter [7].

Next is the management of laser beam energy. The wavelength of the infrared radiation emitted by Nd:YAG and fiber lasers is 1/10^{th} that of CO_2 lasers. This short wavelength results in less reflection and, therefore, high absorbance of radiation, especially if metallic work pieces are used, allowing for even highly reflecting materials to be processed [9]. However, theoretical estimates of the effective absorptivity at the cut front suggest that the shorter wavelength in combination with its high focus ability seems to be primarily advantageous for thin metal cutting, whereas CO_2 laser is probably still capable of cutting thicker materials more efficiently [5]. Thus, for this research, in order to obtain efficient trials for cutting thick material, it is important to understand the management of fiber laser beam energy. Specifically, compared with the results obtained for CO_2 lasers, similar or narrower kerf widths need to be considered.

An important difference between laser welding and laser cutting is that in cutting, generally a portion of the beam passes through the laser–material interaction zone; this is because the cut front inclination varies with speed [7]. In the laser cutting process, cutting speed is an important parameter that decides the heat input in the cutting front and the interaction time of the laser beam work piece (Fig. 1).

At low cutting speeds, as shown in Fig. 2A, the laser/oxygen/steel interaction consists of a cyclic burning reaction. The cut front is almost vertical in this case and is illuminated only by the leading edge of the laser beam, so part of the laser power travels straight through the cut zone without interacting with the material. As the cutting speed is increased, molten material cannot flow out of the cut zone quickly enough to allow the cut front to remain vertical, creating a horizontal lag between the top and the bottom of the cut front. At higher speeds, the cut front becomes less perpendicular, increasing the proportion of the beam that interacts with the cut edge, as depicted in Fig. 2B. In any case, a proportion of the beam is reflected from the cut front [7,10].

Energy input in the process is defined, for a given cut length, by the laser power divided by the cutting speed; within a range of parameters, energy efficiency can be maximized by selecting a larger beam diameter and then minimizing SPE [7].

Finally, kerf width should be taken into consideration. Although compared with other thermal cutting processes, due to small related kerfs, laser cutting generally produces less cutting debris, for the nuclear sector it is important to study this aspect in detail. As stated above, thick metal cutting performance needs to be improved in order to keep the material losses low (which represents nuclear waste) by producing narrow kerf widths [6].

It was reported that increasing the cutting speed decreases the kerf width and roughness of the cut surface, while increasing the power and gas pressure increases the kerf width and roughness [5,11]. In addition, it is known that the presence of oxygen or air leads to a wider kerf; however, a narrow kerf can be obtained using an inert assist gas.

The efficient use of the laser beam in laser cutting requires an understanding of the beam–material interaction, since the resultant kerf width is mainly controlled by the position of the laser focal point (Fig. 3). For high-pressure cutting of stainless steel, the position of the focus should be inside the sheet ($f < 0$) [11].

Studies on basic laser interaction parameters have showed that the “width of weld” in welding is analogous to the “kerf width” in laser cutting. Unlike laser welding, in the cutting case (as Fig. 4 demonstrates) the kerf width is independent of the interaction time. However, the kerf width is mainly controlled by the beam diameter [7].

Hashemzadeh et al. [7] showed that the same thickness can be cut by decreasing SPE and increasing power density. For example, for the same power, decreasing the beam diameter allows the cutting speed to be increased, boosting the cutting efficiency. In addition, the maximum cut thickness can be increased by increasing the power density or SPE, for the same SPE or power density, respectively.

Verhaeghe and Hilton [2] showed that, for a given laser beam quality, a smaller spot will generally produce either a faster welding speed for a given depth of penetration, or an increase in the depth of penetration for a given welding speed. Also, for high power CO_2 laser welding, it was shown that nozzle standoff distance (SD) has a negligible influence on bead width, penetration depth and melted area [4].

The present work aims to analyze the potential of high-power fiber lasers for nuclear power plant decommissioning. The main focus is to achieve higher performance and less waste than are found for Nd:YAG (which have already been studied) or CO_2 lasers.

2. Materials and methods

The experiments involved fixing the laser power and assist gas pressure, and varying the SD and focus position (FP). Measurements

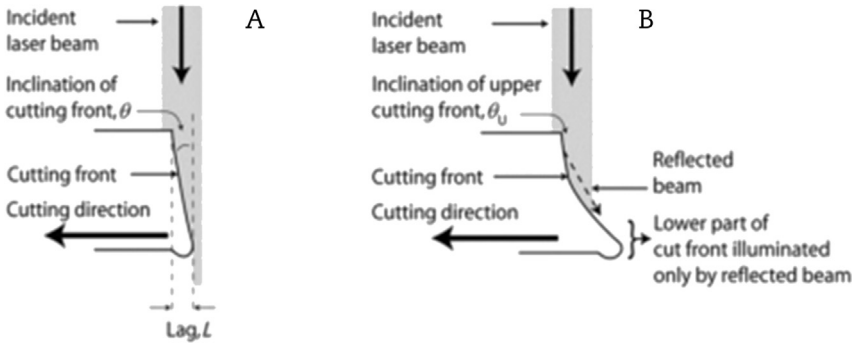

Fig. 1. Cut front laser beam interaction geometries [7].

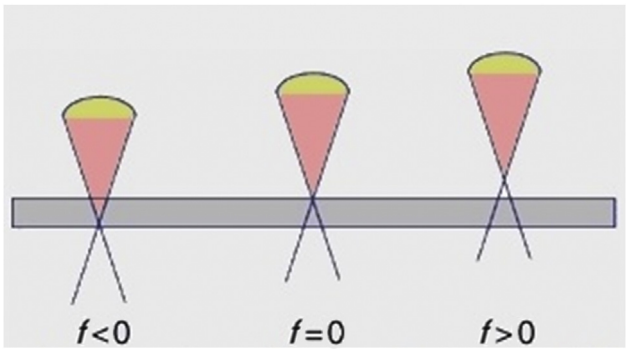

Fig. 2. Illustration of different positions of beam focus with respect to plate surface.

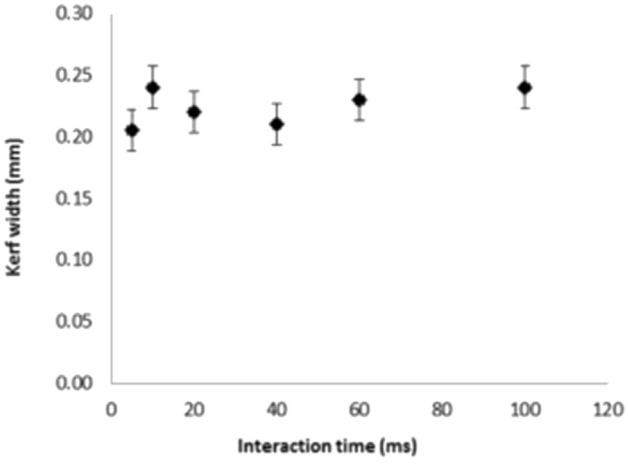

Fig. 3. Kerf width results for cutting sheets of 1 mm thickness [7].

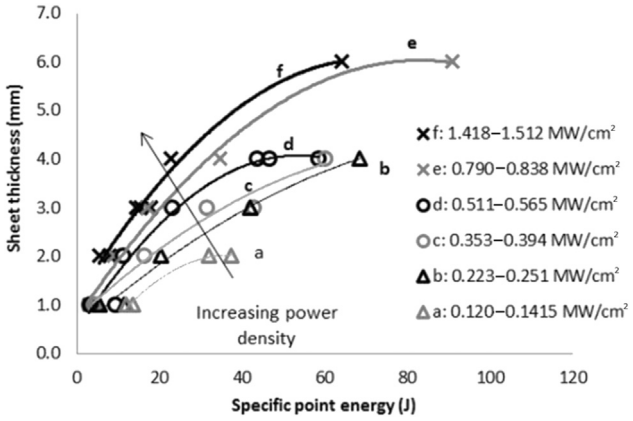

Fig. 4. Maximum cut thickness of the sheet plotted as a function of specific point energy for power density data sets [7].

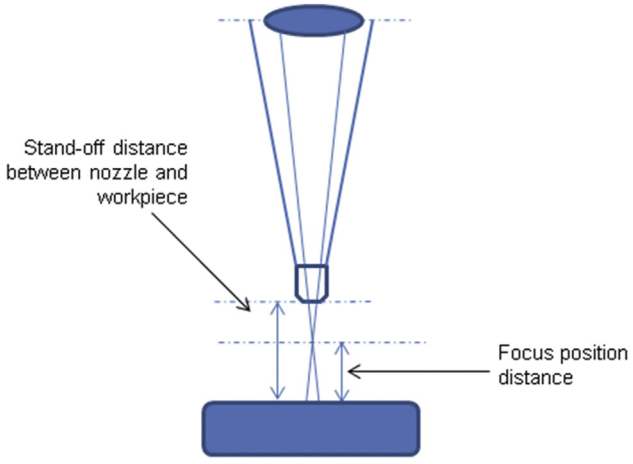

Fig. 5. Definitions of stand-off distance and focus position distance.

were performed with a 10 kW power source and 8 bar gas pressure, for cutting carbon–manganese steel bars with thickness up to 70 mm.

An IPGYLR-10000 fiber laser operating at maximum power was used for the trials. The delivery system consisted of a fiber with a diameter of 200 μm. In the cutting head, the optics consisted of a 120 mm collimator and five lenses of different focal lengths (starting from 250 mm). Using spacer rings, the nozzles were arranged to produce different combinations of SDs and FPs, and to promote different behaviors of the assist gas. Without defocusing the laser beam, seven parameter sets were tested, all with the same nozzle exit design. Fig. 5 shows the definitions of the SD and FP distance.

The material tested was S355 C–Mn steel, widely used in the nuclear sector. Two different experiments were undertaken: for the first experiments, bars of 70 mm thickness were considered suitable, since much deeper cuts are not expected in the nuclear sector. The sequence of cutting speeds was as follows: 1,000 mm/min, 800 mm/min, 600 mm/min, 400 mm/min, 200 mm/min, 100 mm/min, and 50 mm/min. Then, six more cuts were made and an analysis was undertaken, for comparison purposes, with plate thicknesses of 6 mm, 12 mm, and 40 mm, covering the range of thicknesses used in the nuclear sector. The cutting speeds used were 1,200 mm/min, 1,500 mm/min, and 200 mm/min. Chemical composition of the material is presented in Table 1.

Table 1
Chemical composition of S355 C–Mn steel.

Element (wt%) S355 C–Mn steel				
C max	Mn max	P max	S max	Si max
0.20	1.60	0.025	0.025	0.55

After cutting, specimens were prepared from transverse sections; the surfaces were prepared for metallographic inspection by "cold mounting" and polishing to display cross-sectional images of the kerfs. In order to measure the cut areas, different microscopes and measurement software were used.

The trials involved moving of the laser beam from one side of the sample to the other, at a constant speed, in order to discover how deep it can cut, in a single pass, for each speed. After cutting, the kerf width and cut depth produced were measured. The second part of the experiment again involved moving of the laser beam from one side of the sample to the other, at a constant speed. This time, the cuts were used to analyze the cross-section geometries and measure the area cut for different nozzle combinations.

3. Results and discussion

Figs. 6 and 7 show the results of the plots, for each parameter set, of the cut depth and kerf width, respectively, as a function of the corresponding cutting speed. It can be seen that the combinations were able to cut a 70 mm thick section; also, it can be seen that the evolution of the cut depth is similar for each case. However, despite displaying a similar trend, the measured kerf widths revealed different results for each combination.

Looking at Fig. 6, it can be seen that the cut depth is slightly influenced by the SD and FP, with the bigger depths being obtained with FP = 0 mm and FP = −15 m. In addition, the cut depth follows the usual tendency that the depth decreases exponentially with the cutting speed [4].

A detailed look at the kerf width results (Fig. 7), comparing the focal position on the surface of the material (FP = 0) and two

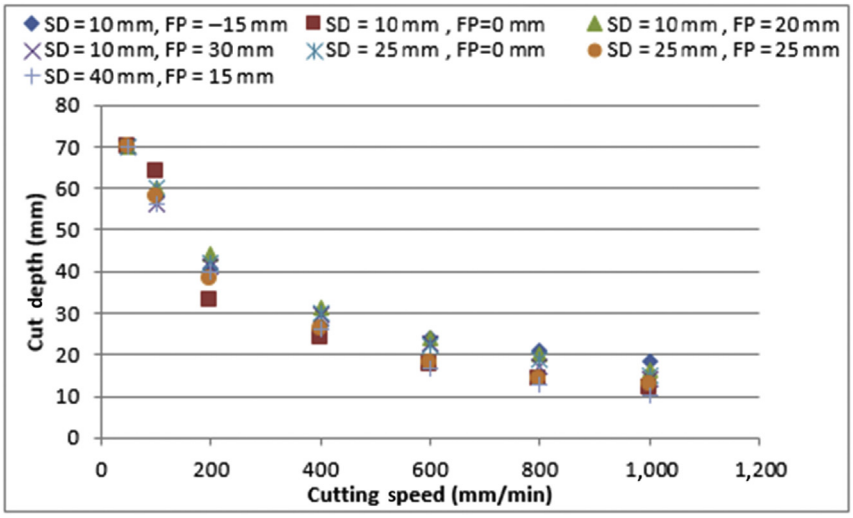

Fig. 6. Cut depth and corresponding cutting speed for each parameter set (for constant power and gas pressure).

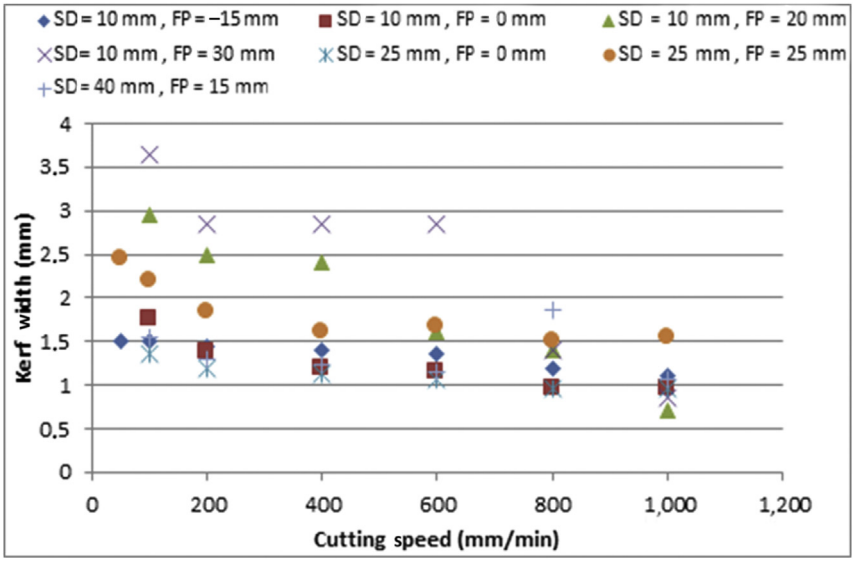

Fig. 7. Kerf width and corresponding cutting speed for each parameter set (for constant power and gas pressure).

Table 2
Two chosen sets of parameters.

1	2
Stand-off distance = 10 mm Focus position = −15 mm Beam diameter = 1.14 mm	Stand-off distance = 25 mm Focus position = 0 mm Beam diameter = 0.36 mm

different values of SD, shows that different SDs do not influence the obtained results, indicating high tolerance of the laser cutting process used to this parameter, as was also concluded by Hilton et al. [6]. Similarly, independent of the SD, lower kerf widths are obtained for the smallest FP. Thus, the factor that appears to significantly affect the kerf width is the focal point position, which represents different beam diameters.

Moreover, Fig. 7 shows that for SD = 10 mm, use of the minimum spot size on the surface of the material (FP = 0) or below the work-piece surface (FP = −15) results in a narrower kerf width. Similarly, with SD = 25 mm, it can be observed that the focal point position on the surface of the material produces a smaller kerf width than is produced with a beam focusing above the work-piece surface.

Considering the narrower kerfs mentioned above, two corresponding parameter sets were used for further analysis (Table 2). These sets are able to produce narrower kerfs, for the same thickness, in cases of using CO_2 or other ND:YAG lasers [1, 12].

The different laser systems will be compared based on the SPE concept, referred to in the Introduction section.

Variation of the maximum cut depth was plotted, for the speed involved, as a function of SPE. A comparison of Figs. 5 and 8 shows that SPE analysis can be applicable to laser cutting within the parameters used in this study.

Fig. 9 shows that it is possible to cut up to 70 mm using both conditions. In addition, for the same power density, thickness of the cut material increases with increasing SPE. It can be seen that the same thickness can be cut by decreasing SPE, which represents a decrease in the interaction time or, in this study, the beam diameter at the surface of the material.

In welding, the weld width, for a given weld penetration depth, was previously reported as being mainly controlled by the interaction time, whereas in laser cutting the kerf width is mainly controlled by the beam diameter [7]. In this case, the kerf width is slightly dependent on the interaction time. Comparing these cuts, it can be seen that both the smallest and the largest beam diameters lead to similar maximum kerf widths. It is important to report that, for both combinations, the maximum kerf width obtained is

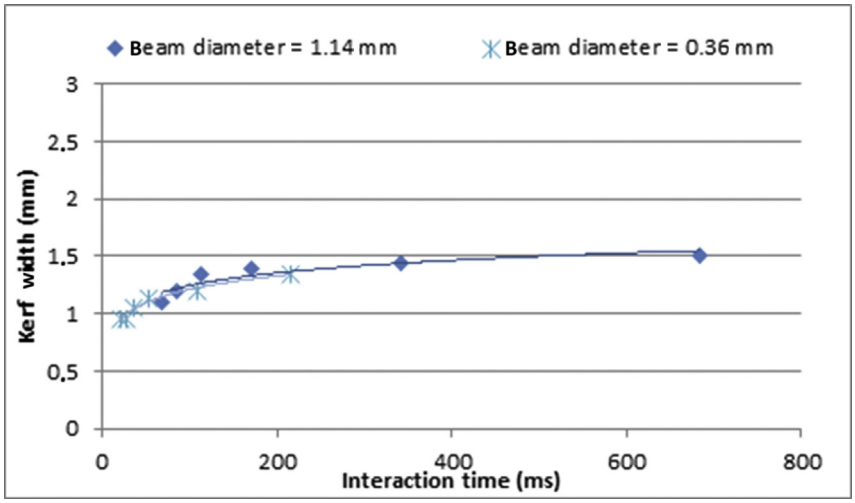

Fig. 8. Kerf width (for the parameters used in each case) as a function of interaction time.

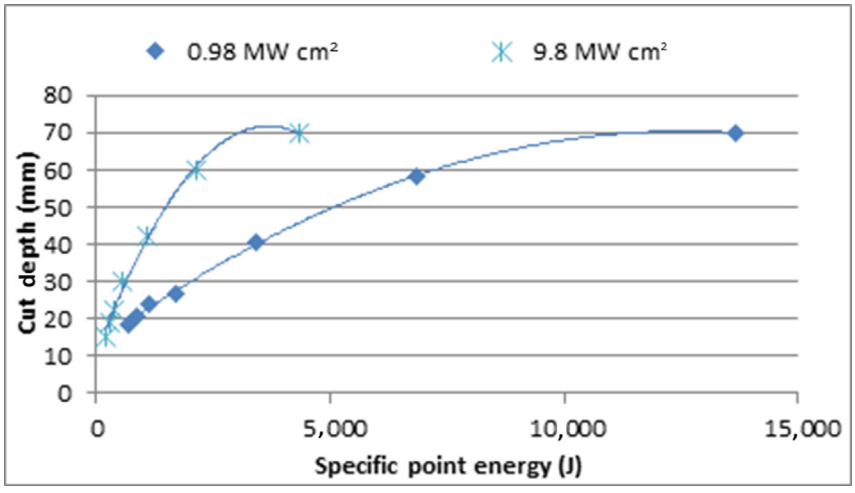

Fig. 9. Maximum cut thickness (for the parameters used in each case) as a function of specific point energy.

narrower (of the order of 20% narrower) than those obtained in other studies for the cutting of thick materials [1]. Moreover, Fig. 8 shows that, after a certain interaction time (100 milliseconds), independently of the beam diameter, decreases in the cutting speed do not influence the kerf width.

The kerf cross section and the measured "cut area" resulting from the second part of the experiment are shown in Fig. 10. The figure shows that similar kerfs can result in different material removal rates. For thinner materials (6 mm and 12 mm), the area is close, within the experimental error, for the two different sets. For thick plates, the difference is significant: the experiment with the minimal focal spot on the work-piece surface presents removal of more materials for the same speed.

A rectangular cutting geometry is related to the distance between the nozzle and the surface of the work piece [13]. The use of different SDs results in similar kerf widths and cut depths; from an

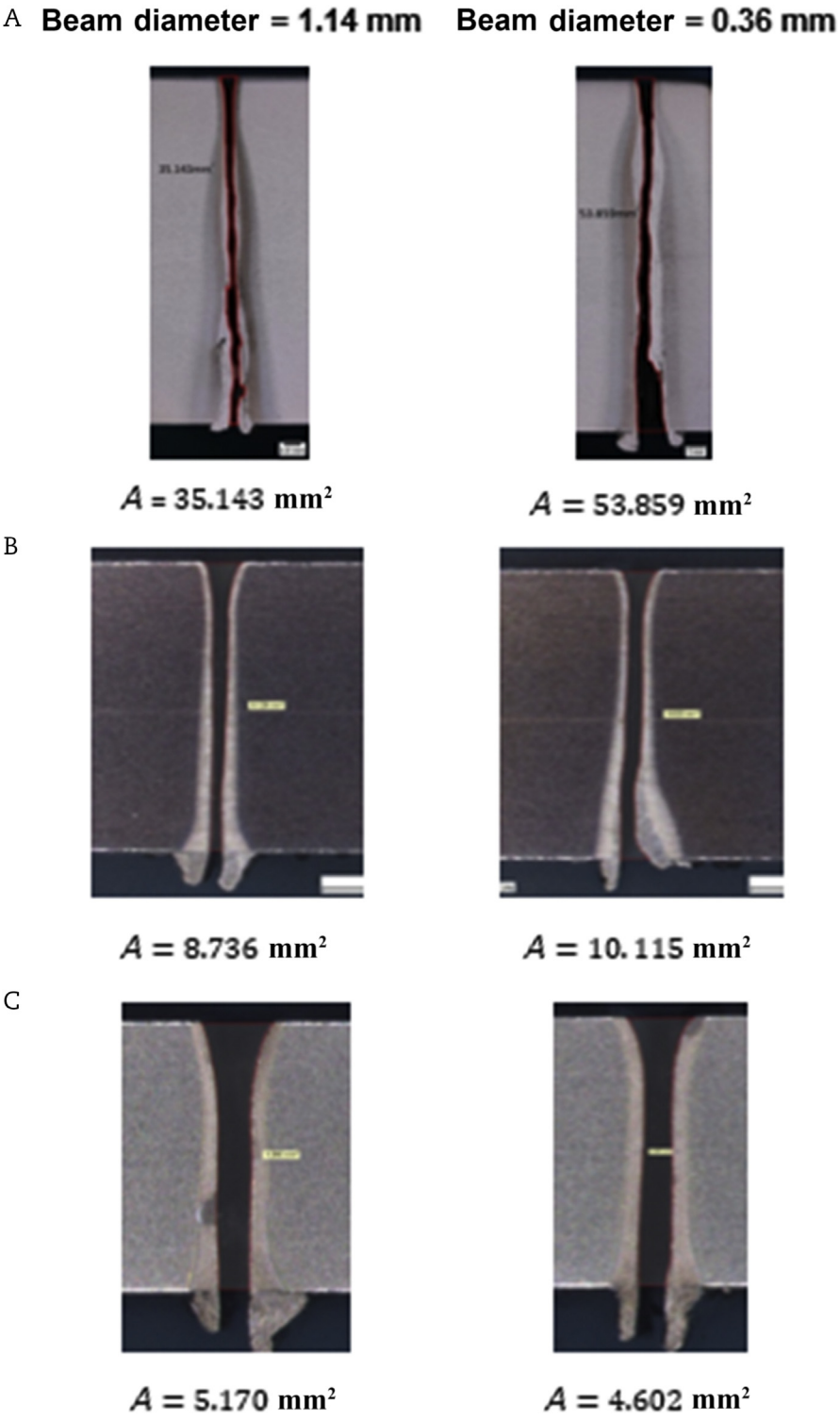

Fig. 10. Kerf cross section and "cut area" measures for C–Mn steel of various thickness. (A) 40 mm. (B) 12 mm. (C) 6 mm.

observation of the cut area it seems that the geometry is dependent on this distance. This influence can be explained by the speed rate of the assistant gas, which becomes lower for higher SDs. However, because, in the nuclear sector, in this type of work, the capability to sever the material is more important than the ability to maintain the cut quality [6], this parameter was not considered.

In turn, the difference in the geometry for each thickness is due to the vaporization that occurs at low speeds [13]. A high-energy input results in an intense material removal, which results in irregular kerfs.

The material removal rate can be considered as the product of the kerf cross-sectional area and the cutting speed. The calculated material removal values for different FPs are presented in Fig. 11. For a constant FP, Fig. 11 shows that the thicker material generates lower "volume removed per minute", which is explained by the slower cutting speed needed to cut the material. However, a higher rate can be seen for 12 mm thickness, possibly due to the high speed used. Globally, the minimum rate is achieved using a focal position inside the surface of the material. This difference could be explained by the portion of the beam that does not interact with the material, at low cutting speeds, which appears to be higher for the experiment with the minimal focal spot on the work-piece surface. In addition, the results could be slightly influenced by the attached dross inside the cut area, which was not measured.

Using the same criteria as those used in Fig. 8, the section removed per minute was plotted as a function of the interaction time; the results are shown in Fig. 12. It can be seen that, for both diameters, the removed area increases with the interaction time. In agreement with the previous results (Fig. 11), it is also shown that the smallest beam diameter leads to higher performance, which translates into greater material removal for the same cutting speed.

4. Conclusion

High-power fiber laser is a promising cutting tool for decommissioning of nuclear reactors. The objective of this experimental study was to assess the performance of a 10 kW laser for thick sections. To minimize detrimental effects, the procedures were characterized as follows: (1) The cut depth is not significantly influenced by different nozzle combinations. (2) The factor that appears to affect the kerf width most significantly is the focal position. Minimum laser spot diameters are thus advised for smaller kerf widths. (3) The same thickness can be cut by decreasing the beam diameter. However, after a certain interaction time, the beam diameter does not influence the kerf width. (4) For constant laser

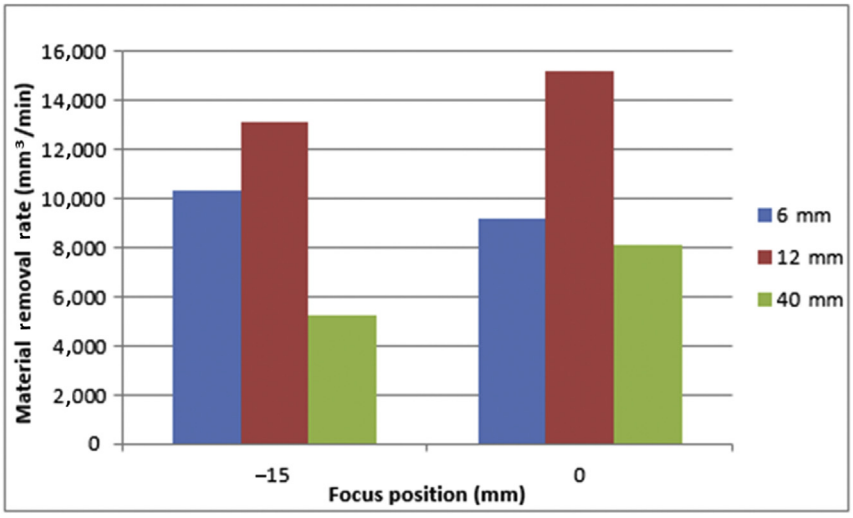

Fig. 11. Material removal rate as a function of focal positions for C–Mn steel of 6 mm, 12 mm, and 40 mm thickness.

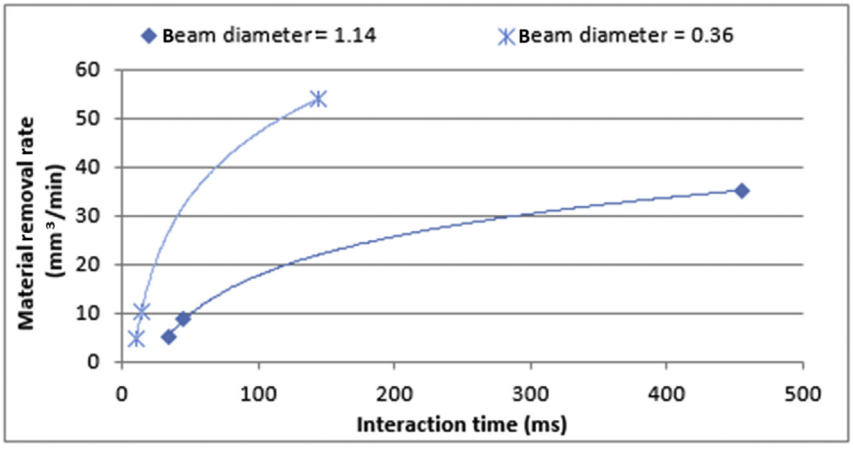

Fig. 12. Material removal rate as a function of interaction time.

power and cutting speed, focusing the laser beam below the surface of the material results in less material removal for the same interaction time.

Disclaimer

The results described in this paper were generated at TWI Ltd, as part of the LaserSnake2 collaborative research project, whilst the primary author was on secondment. LaserSnake2 is co-funded by Innovate UK, the Department of Energy and Climate Change, and the Nuclear Decommissioning Authority, under Grant number 110128. The LaserSnake2 project includes OC Robotics, TWI Ltd, Laser Optical Engineering, ULO Ltd and the UK's National Nuclear Laboratory.

Conflicts of interest

All authors have no conflicts of interest to declare.

References

[1] C. Chagnot, G. De Dinechin, G. Canneau, Cutting performances with new industrial continuous wave ND: YAG high power lasers: for dismantling of former nuclear workshops, the performances of recently introduced high power continuous wave ND: YAG lasers are assessed, Nucl. Eng. Des. 240 (2010) 2604–2613.

[2] G. Verhaeghe, P. Hilton, The Effect of Spot Size and Laser Beam Quality on Welding Performance When Using High-power Continuous Wave Solid-state Lasers, ICALEO, 2005.

[3] B.S. Yilbas, Laser cutting of thick sheet metals: Effects of cutting parameters on kerf size variations, J. Mater. Process. Technol. 201 (2008) 285–290.

[4] L. Quintino, A. Costa, R. Miranda, D. Yapp, V. Kumar, C.J. Kong, Welding with high power fiber lasers—a preliminary study, Mater. Des. 28 (2007) 1231–1237.

[5] A. Mahrle, E. Beyer, Theoretical aspects of fibre laser cutting, J. Phys. D. Appl. Phys. 42 (2009) 175507.

[6] P.A. Hilton, A. Khan, R. Buckingham, Advances in Laser Cutting as a Decommissioning and Dismantling Tool Laser Cutting of Plate Material, TWI internal report. (2015) 1–6.

[7] M. Hashemzadeh, W. Suder, S. Williams, J. Powell, A.F.H. Kaplan, K.T. Voisey, The application of specific point energy analysis to laser cutting with 1 μm laser radiation, 8th International Conference on Photonic Technologies, LANE, 2014, Physics Procedia 56 (2014) 909–918.

[8] E. Assuncao, S. Williams, D. Yapp, Interaction time and beam diameter effects on the conduction mode limit, Opt. Lasers Eng. 50 (2012) 823–828.

[9] H.A. Eltawahni, M. Hagino, K.Y. Benyounis, T. Inoue, A.G. Olabi, Effect of CO_2 laser cutting process parameters on edge quality and operating cost of AISI316L, Opt. Laser Technol. 44 (2012) 1068–1082.

[10] J. Powell, S.O. Al-Mashikhi, A.F.H. Kaplan, K.T. Voisey, Fibre laser cutting of thin section mild steel: an explanation of the 'striation free' effect, Opt. Lasers Eng. 49 (2011) 1069–1075.

[11] W.P. Jüptner, LIA handbook of laser materials processing, Opt. Lasers Eng. 38 (2002) 608–610.

[12] P.A. Molian, Dual-beam CO_2 laser cutting of thick metallic materials, J. Mater. Sci. 28 (1933) 1738–1748.

[13] R. Pfeifer, D. Herzog, M. Hustedt, S. Barcikowski, Pulsed Nd :YAG laser cutting of NiTi shape memory alloys—influence of process parameters, J. Mater. Process. Technol. 210 (2010) 1918–1925.